Fine Chemical Engineering
https://ojs.wiserpub.com/index.php/FCE/

Research Article

C_6 to C_{17} Organic Products from Artificial Photosynthesis Catalyzed by 2-Phenyl Indole (PI) Titanium Tetrachloride Complex $(PI)_2TiCl_4$: The Synergism of Hydroxyl Radicals

Gregory G. Arzoumanidis[1*], **Michail Paraskevas**[2]

[1]Oakwood Consulting, Inc. Naperville, IL, 60540, USA
[2]Guangdong Technion Israel Institute of Technology, Jinping, Shantou, Guangdong, 515063, P. R. China
E-mail: arzoumandis@gmail.com

Received: 13 December 2024; **Revised:** 18 February 2025; **Accepted:** 27 February 2025

Graphical Abstract:

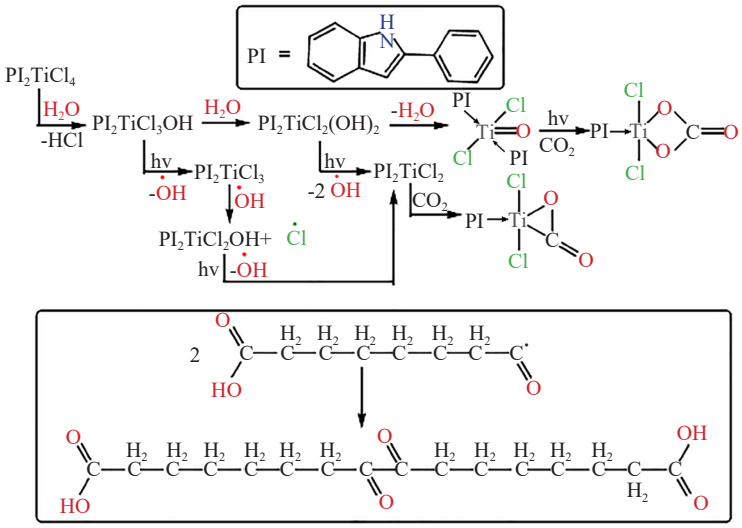

Abstract: The newly discovered artificial photosynthesis process catalyzed by 2-phenyl indole (PI) and $TiCl_4$ complexes, activated by visible light, produces long-chain oxygenated hydrocarbons up to C_{17}. This process begins with the formation of α-carboxylic acid-ω-aldehyde compounds (C_6 to C_9), arising from a cascade of autocatalytic organotitanium complexes derived from $(PI)_2TiCl_4$. These complexes are formed via hydrolysis through ambient air humidity and the direct atmospheric capture (DAC) of CO_2. Carbon chain growth utilizes system-generated formaldehyde as a feedstock. The initial C_6 to C_9 compounds can further couple into C_{12} to C_{17} derivatives through a radical mechanism initiated by hydroxyl radicals. A proposed mechanism explores the synergistic interaction between organotitanium catalysis and hydroxyl radicals. This development represents the only known heterogeneous catalytic

DOI: https://doi.org/10.37256/fce.6120256245

system that autonomously captures CO_2 and humidity from the atmosphere to subsequently produce long-chain oxygenated hydrocarbons using solar energy.

***Keywords*:** artificial photosynthesis, photocatalysis, organotitanium complexes, CO_2 capture, hydroxyl radicals

1. Introduction

Most artificial photosynthesis (AP) systems, including those at the forefront of research, focus on water splitting for hydrogen production or reducing CO_2 to basic hydrocarbons (C_1-C_3). The ability to synthesize long-chain compounds (up to C_{17}) offers a transformative opportunity to produce higher-value chemicals, advancing AP technology scalability.

The newly developed $TiCl_4$/2-phenylindole (PI) photocatalytic system uses visible light to convert atmospheric CO_2 and H_2O into multi-carbon oxygenated hydrocarbons.[1] This breakthrough integrates Direct Air Capture (DAC) of CO_2 with conversion, addressing critical challenges in climate change, energy sustainability, and resource efficiency.

The mechanism involves forming photoactive Ti^{4+}-OH bonds through the hydrolysis of Ti^{4+}-Cl bonds by ambient air humidity. Upon exposure to light and air, these Ti^{4+}-OH bonds release hydroxyl radicals,[2-3] facilitating the reduction of the titanium center ($Ti^{4+} \rightarrow Ti^{3+}/Ti^{2+}$). The reduced titanium species, with increased electron density, effectively capture atmospheric CO_2, initiating a spontaneous and intricate reduction process that produces long-chain oxygenated hydrocarbons. This solar-driven, autonomous production distinguishes the system from conventional AP methods.

Traditional AP approaches primarily target water splitting and CO_2 reduction to small hydrocarbons (C_1-C_3) using metal oxide catalysts. These methods often require high CO_2 concentrations[4] and separate processes, achieving limited success. In contrast, the novel organotitanium-based system integrates water splitting[5] and CO_2 reduction into a single, continuous process, producing oxygenated organics directly from ambient CO_2 (~0.04%). This capability to convert trace amounts of CO_2 into valuable materials represents a significant leap in AP technology.

A crucial feature of this system is the photocatalytic generation of hydroxyl radicals released from Ti^{4+}-OH, Ti^{3+}-OH, and Ti^{2+}-OH bonds. With a redox potential of 2.8 V (second only to fluorine), hydroxyl radicals are highly reactive, yet transient species that drive the organotitanium catalytic process. While TiO_2 photocatalysis[6] is known to produce hydroxyl radicals,[7] their synergistic role in facilitating complex reaction cascades in this system is unprecedented.

Although hydroxyl radicals typically exist on the nanosecond scale, they can persist for up to 600 seconds in aqueous environments, enabling diverse redox reactions. These include dimerization to form H_2O_2, oxidation of Ti=O bonds to peroxo-titanium species (Ti-O-O), oxidation of PI ligands to N-O functionalities, conversion of CO_2 to HCOOH, and condensation or radical coupling involving formaldehyde-derived intermediates.

The autonomous, multi-step nature of this system-driven by hydroxyl radical-mediated pathways-highlights its efficiency and versatility. Understanding these transformations is essential for optimizing or tailoring the system for specific goals, such as oxygen production via hydroxyl radical dimerization, where pH significantly influences outcomes.

This system's ability to sustain multiple valuable reactions in a continuous process, especially DAC and CO_2 reduction, underscores its transformative potential. Further investigation into its mechanism could unlock even greater industrial and environmental applications.

2. Results and discussion

2.1 *Focus*

The aim of this research article is to identify the C_6 to C_{17} oxygenated hydrocarbons produced by the PI/$TiCl_4$ photocatalytic system, propose the mechanism of their formation, determine their relative concentration, and discuss the role of hydroxyl radicals using experimental Matrix-Assisted Laser Desorption Ionization-Time of Flight Mass Spectrometry (MALDI-TOF MS) data.

The direct conversion of atmospheric carbon into complex, long-chain organic molecules advances green chemistry and renewable energy goals. The visible-light-activated organotitanium complexes exhibit self-organizing behavior,

forming autocatalytic reaction networks. These networks drive three self-sustaining cycles, where reaction products catalyze subsequent reactions, showcasing an innovative approach to sustainable molecular assembly.

2.2 *First catalytic cycle*

In the first photocatalytic cycle, the $(PI)_2TiCl_4$ complex is the essential "starter" catalyst, initiating a self-organized cascade. This complex interacts autonomously in the solid state with environmental inputs-visible light, H_2O, and CO_2-evolving into a sophisticated, multi-component photocatalytic system. Similar photocatalytic behavior has been observed in titanium click chemistry[8] studies.

The process begins with the hydrolysis of $(PI)_2TiCl_4$ by atmospheric moisture,[9] forming intermediate complex **1**, which converts to complex **2** (see Figure 1). Under visible light, Complex **1** reacts with CO_2, forming organotitanium carbonate complex **10** (illustrated in Figure 2), while Complex **2** releases hydroxyl radicals, generating Ti^{2+} complex **3**. Complexes **1** and **3** capture atmospheric CO_2 (0.04%), a significant advance for climate change mitigation research.

Complex **4** coordinates with system-generated CO, replacing a PI ligand to form complex **8**. This coordination facilitates CO insertion into the Ti-C bond, yielding the unique titanium α-ketocarboxylate complex **9**. The four-membered Ti-O-C-C titanaoxetane ring structure, previously observed[9] in rhodium, silver, and other metals, appears for the first time in titanium chemistry as a ketocarboxylate ring.

Alternatively, complex **4** undergoes hydrolysis to form Complex **5**, which, upon irradiation, releases hydroxyl radicals and transforms into complex **6**. This complex then rearranges into formaldehyde coordination complex **7**, by reacting with the newly released hydroxyl radicals.

The carbonate Complex **10** (Figure 2), formed from activated complex **1** and captured atmospheric CO_2, can generate formaldehyde (complex **12**) and/or methanol (complex **13**) through a hydrogenation mechanism. Hydrogen is produced internally via photocatalytic water splitting.[4] The continuous catalytic cycle shown in Figure 2, incorporating DAC of CO_2, provides a sustainable source of formaldehyde and methanol as valuable feedstocks.

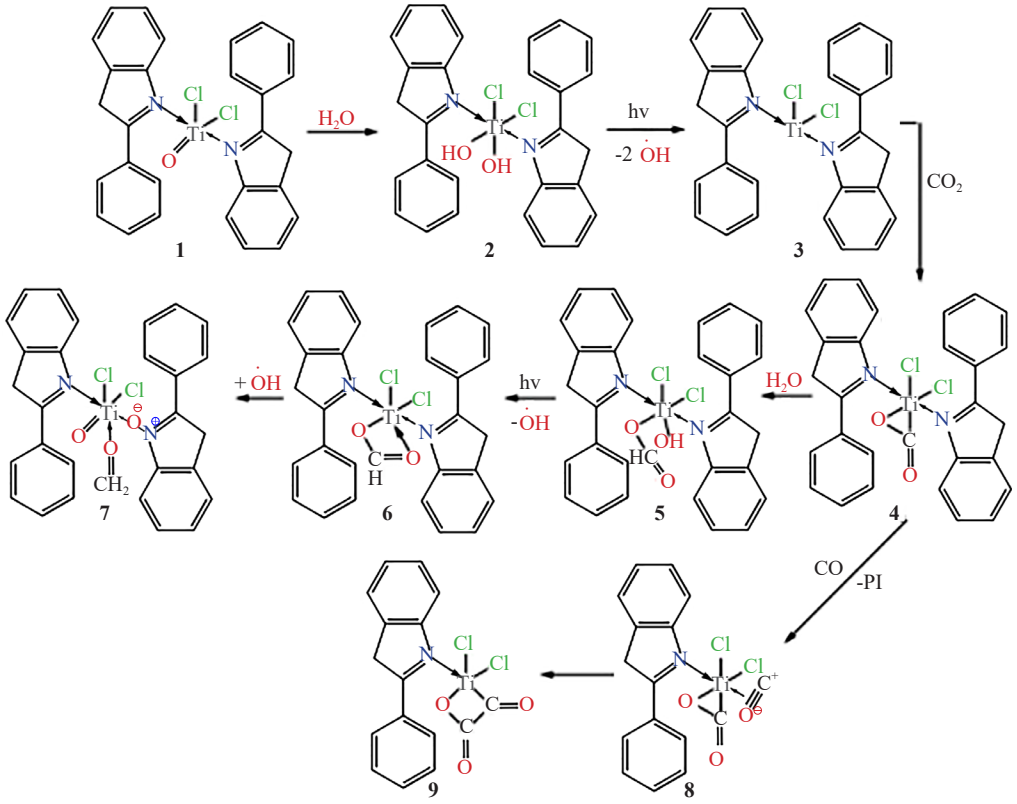

Figure 1. Initiation of the photocatalytic process based on $(PI)_2TiCl_4$

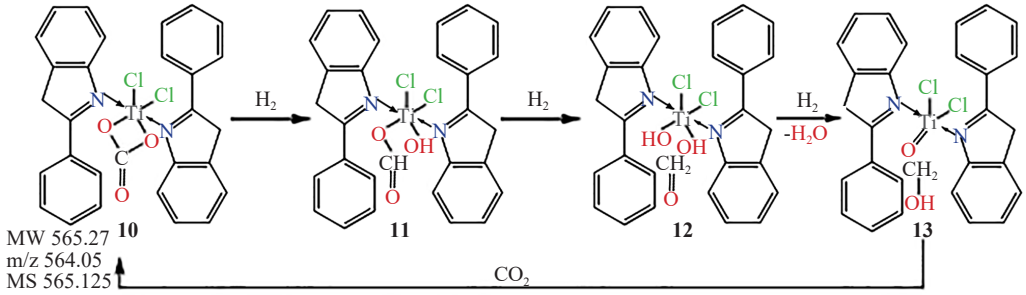

Figure 2. The hydrogenation of carbonate Complex **10** yields formaldehyde (Complex **12**) and/or methanol (complex **13**)

2.3 *Second catalytic cycle*

The tetrahydrofuran (THF)-coordinated analog of complex **9**, identified as complex **14** (Figure 3) in MALDI-TOF analysis, initiates a new cycle in the cascade process, aiding the formation of long-chain organics. It uses formaldehyde as a building block, leading to the formation of Complexes **15**, **16**, and **17**. The THF coordination in Complexes **14**-**17** is specific to the experimental conditions, as these were conducted in THF. In the absence of THF, Complex **9** is expected to coordinate directly with formaldehyde.

The α-ketocarboxylate complex **14** undergoes a photocatalytic transformation to form ketene Complex **15** and cumulene derivative **16** through a condensation with formaldehyde. The reaction involves dehydration via H_2O elimination.While not detected by MALDI-TOF, it appears that a third condensation step occurs, contributing to the partially hydrogenated Complex **17**. The PI oxygenated analog of **17** is Complex **21** (Figure 6), which is crucial in the third and final catalytic cycle.

Titanium in Complex **14** is highly electrophilic due to the electron-withdrawing chloride ligands and the carbonyl moieties of the titanaoxetane ring.[10] This allows formaldehyde, with its nucleophilic oxygen, to react readily with the titanium center, forming Complex **18** (Figure 4).

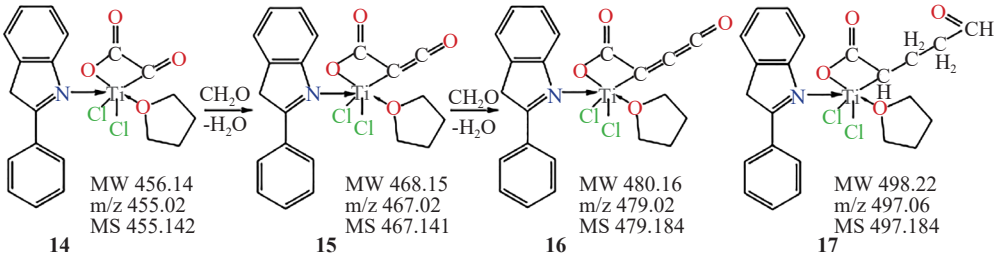

Figure 3. Photocatalytic conversion of the *α*-ketocarboxylate Complex **14** results in ketene **15** and cumulene derivative **16** via an apparent formaldehyde condensation with a keto group, accompanied by H_2O elimination. The hydrogenated Complex **17** likely originates from a related intermediate, featuring a pendant carbon chain with three carbon atoms

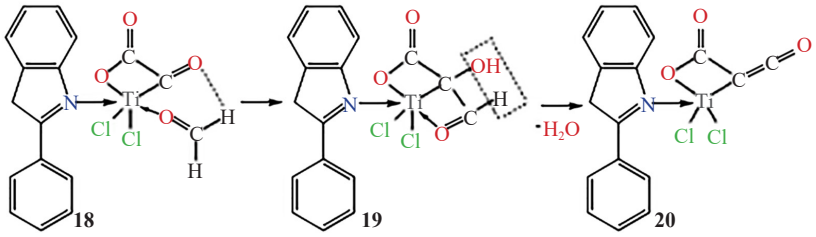

Figure 4. Aldol-type condensation of formaldehyde coordinated to titanium, leading to dehydration and formation of ketene Complex **20**

The second catalytic cycle begins with Complex **14**, which initiates a novel formaldehyde condensation process, driving the formation of long-chain organic molecules through a series of orchestrated steps outlined below:

(1) Formation of Ketene: An Aldol condensation occurs between formaldehyde and the carbonyl group of Complex **14**, facilitated by the coordination of formaldehyde to titanium, as shown in Figure 4.

(2) Repeating Reactions: The Aldol condensation proceeds iteratively, forming Complex **16** with a cumulene side chain. While formaldehyde could theoretically react further with Complex **16** to produce a compound containing four consecutive double bonds, such structure would be intrinsically unstable. Nonetheless, evidence for the transient existence of such intermediate is supported by the detection of hydrogenated Complex **17**, characterized by a side chain of three carbon atoms, terminating in a reactive aldehyde group.

Again, the reaction sequence of the second cycle underscores the central role of Complex **9** (or the analogous THF coordinated **14**) as the initiating catalyst and driver, achieving long-chain organic molecule production.

2.4 *MALDI-TOF MS data*

The structures of catalytic intermediates formed through the cascade transformations of the original $(PI)_2TiCl_4$ complex were primarily elucidated via Matrix-Assisted Laser Desorption Ionization-Time of Flight Mass Spectrometry (MALDI-TOF MS), which has proven highly effective in characterizing transition metal catalysts.[11,12] MALDI-TOF is particularly advantageous for identifying intact metal complexes. Besides MALDI-TOF, the detailed process of deciphering this dynamic chemical system's cascade sequence and verifying individual complexes and other products was supported by other key observations as well:

(a) Comparative reactivity analysis of similar organotitanium systems, including hydroxyl radical formation by a substituted ansa-titanocene dihydroxido complex under daylight irradiation[2,3] and the established ability of titanium oxo (Ti=O) groups to convert to peroxo species (Ti-O-O-) upon H_2O_2 exposure; (b) Observations of ordered reaction sequences across multiple cycles of the photosynthetic cascade, as illustrated in Figures 1 and 2; (c) Expected formation of trichloro-and dichloro-titanium PI complexes upon daylight-induced reduction of the titanium tetrachloride PI coordination compound.[12]

Complexes in Figure 2 and Figure 3 are labeled with calculated molecular weights (MW) and expected m/z ratios, which reflect the natural isotopic distribution of the elements in each complex, along with the experimentally recorded MALDI-TOF MS data. The close match between calculated (MW, m/z) values and the experimental MS data strongly supports the structural identity of each complex.

Figure 5 displays the MALDI-TOF spectrum in CH_2Cl_2 for a $(PI)_2TiCl_4$ complex exposed to air and daylight over three weeks, highlighting C_6 to C_{17} oxygenated organic products. Their identities are discussed in detail and their relative concentrations on a scale of 0-7 are represented by the peak intensities in the MALDI-TOF spectrum, summarized in Table 1. The identification of the organotitanium catalytic intermediates was addressed in our previous publication,[1] which includes Figure 5.

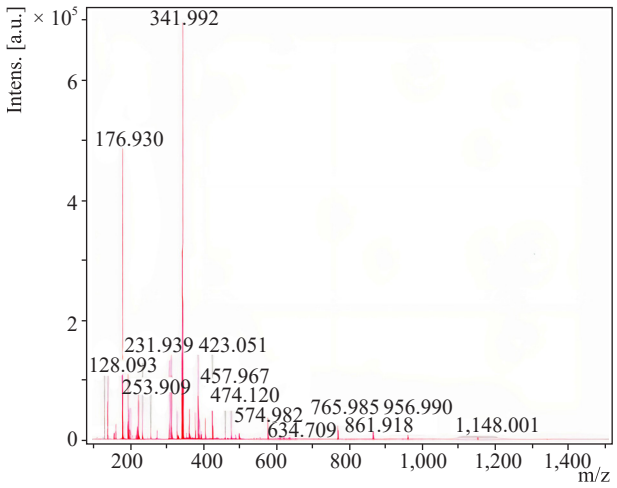

Figure 5. Maldi-T of spectrum in CH_2Cl_2 featuring organic products from artificial photosynthesis catalyzed by $(PI)_2TiCl_4$

Remarkably, 54% of the final C_6 to C_{17} mix constitutes C_{16} products. Also, the calculated C_8 original concentration (before the radical coupling of the initial C_6 to C_9 products) is 72.5%. The reason for the high C_8/C_{16} concentration is unknown and should be further investigated.

Table 1. Percent relative concentrations of C_6 to C_{17} oxygenated hydrocarbon products

					% Total Original* Concentrations			
Nu	MS	C_x	Relative Intensity	%	C_6	C_7	C_8	C_9
1	128.093	C_6	0.1	0.45	0.65	21.23	72.50	6.62
2	140	C_7	1.1	5.0				
3	152	C_8	0.2	0.9				
4	156	C_8	0.4	1.8				
5	176.930	C_7	4.8	21.9				
6	193	C_7	1.1	5.0				
7	199	C_9	0.2	0.9				
8	216	C_9	1.3	5.9				
9	231.939	C_9	0.2	0.9				
10	253.909	C_{12}	0.1	0.45				
11	272	C_{13}	0.2	0.9				
12	306	C_{16}	1.4	6.4				
13	313	C_{16}	1.4	6.4				
14	328	C_{17}	0.4	1.8				
15	341.992	C_{16}	6.9	31.5				
16	358	C_{16}	0.4	1.8				
17	378	C_{16}	0.3	1.4				
18	382	C_{16}	1.4	6.4				

* Calculated, before radical coupling

2.5 *Third catalytic cycle*

The cascade operation continues with a third cycle, as shown in Figure 6. It begins with the N-oxidation of the PI ligand in Complex **17**, most likely facilitated by hydroxyl radicals, forming Complex **21**. This new sequence introduces a unique formaldehyde condensation process involving the aldehyde group on the side chain of the organotitanium complexes. This leads to the consecutive formation of Complexes **22**, **23**, and **24**, marking another step in the cascade transformation.

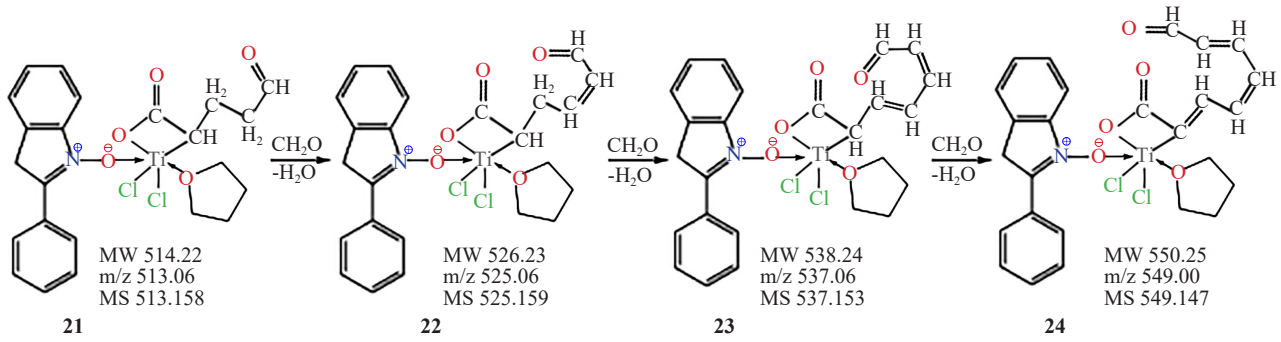

Figure 6. Third catalytic cycle. New-type condensation of formaldehyde with the aldehyde group of the side chain on organotitanium complex **21**. Consecutive carbon addition and double-bond creation on the side chain, from Complex **21** to Complex **24**

A breakdown of the third cycle highlights the following key steps:

(1) N-Oxidation: Complex **17** undergoes N-oxidation by hydroxyl radicals to form complex **21**, initiating the third cycle.

(2) Condensation with Formaldehyde: Complex **21** reacts with formaldehyde, forming complex **22**, which undergoes two further condensations to yield complexes **23** and **24**.

(3) Carbon Chain Growth: Each condensation extends the carbon chain, adding a unit and creating conjugated double bonds. The process halts when the double bond reaches the titanaoxetane ring in complex **24**.

(4) Formation of Unsaturated α-Carboxylic Acids-ω-Aldehydes: Complexes **22**. **23**, and **24** serve as precursors to C_6, C_7, and C_8 unsaturated α-carboxylic acids-ω-aldehydes, respectively, see below. These compounds are produced autonomously by the system from their respective organotitanium complexes, by an apparent hydrolysis.

(5) Potential for Further Growth: The linear carbon chains can further grow up to C_{17}, by a radical coupling process initiated by hydroxyl radicals. Additional details are provided later in the text.

The third cycle reaction sequence illustrates a novel formaldehyde condensation mechanism, enabling complex organotitanium structures to autonomously generate unsaturated α, ω-carboxylic acids-aldehydes. This process exhibits significant potential for additional carbon chain growth and radical coupling reactions. These advancements further underline the system's ability to construct intricate organic frameworks, offering transformative insights into organotitanium chemistry and catalytic cascade design, which will be elaborated upon in subsequent sections.

2.6 *Hydroxyl radicals-assisted reaction of aldehyde with formaldehyde*

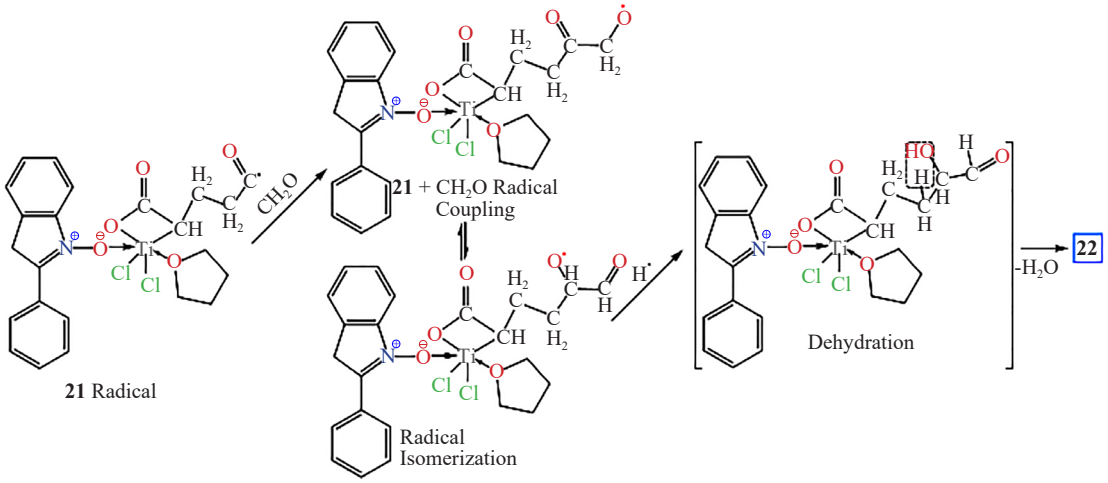

Figure 7. Mechanism of the photocatalytic coupling of CH_2O with Complex **21** Radical. Isomerization, hydrogenation, and dehydration of transient intermediate to yield Complex **22**

The systematic "carbon growth" with system-produced formaldehyde as the building block is most likely related to the titanium photocatalyzed radical coupling of formaldehyde with methanol.[13] Hydrogen abstraction from the aldehyde side arm of Complex **21** induced by hydroxyl radicals will create the corresponding **21**-radical complex (Figure 7). This radical couples with formaldehyde, creating a **21** + CH_2O radical intermediate, which isomerizes into an alcohol/aldehyde radical. Via hydrogen atom transfer (HAT) from hydroxyl radicals, a dehydration intermediate forms. Subsequent dehydration yields the conjugated double bond seen in Complex **22**, showcasing an orderly mechanism for chain extension.

2.7 *Formation of C_6 to C_9 oxygenated hydrocarbons*

The hydrolytic separation of Complexes **22**, **23**, and **24** yields three primary organic products, identified by MALDI-TOF as MS 128.093, MS 140, and MS 152, respectively (Figure 8). These products correspond to distinct stages of the chain-growth process. Furthermore, these intermediates demonstrate versatility through subsequent transformations, such as acid-catalyzed double-bond hydration, producing a hydrated derivative (MS 176.93), or partial hydrogenation, yielding MS 156. These pathways highlight the catalytic system's capability to generate a diverse array of organic molecules through targeted modifications of the initial products.

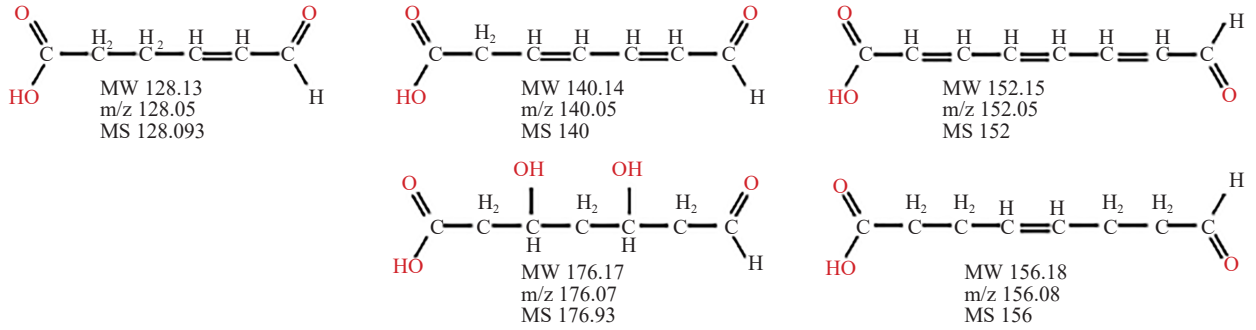

Figure 8. α, ω-Cx carboxylic acid-aldehyde unsaturated organics (x = 6, 7, 8), identified as MS 128.093, 140, 152, generated by hydrolysis from Complexes **22**, **23**, **24**, respectively. Second Row: Corresponding hydrated (MS 176.93) and partially hydrogenated (MS 156) products

The MALDI-TOF MS data points 199, 216, and 231.939 correspond to three sequentially hydrated C_9 unsaturated organic compounds, as illustrated in Figure 9. These structures are identified as hydrated derivatives of a parent C_9 unsaturated α-carboxylic acid-ω-aldehyde compound. However, the exact formation mechanism of this parent compound remains unclear and could not be conclusively determined. This ambiguity underscores a critical gap in understanding the cascade reaction process, necessitating further investigation into the pathways responsible for the generation of these hydrated organic derivatives.

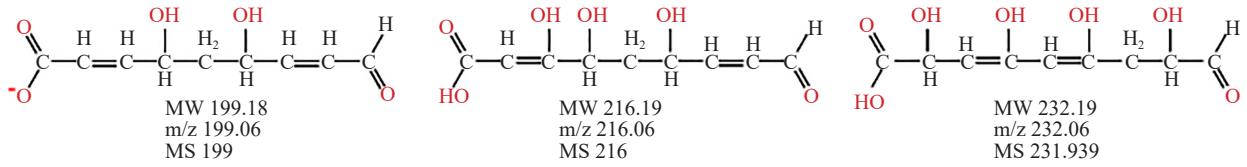

Figure 9. MALDI-TOF identified C_9 oxygenated derivatives

The organic products corresponding to MS 216 and MS 231.939, both C_9 unsaturated derivatives, are involved in coupling reactions with a PI radical. In these reactions, the PI radical facilitates the extension or functionalization of the C_9 framework.

2.8 *Creation of C_{12} to C_{17} and PI coupling products: the essential role of hydroxyl radicals*

The next category of products includes C_{12} to C_{17} linear carbon chains with a notably high concentration of C_{16} organics. The conspicuous absence of C_{10} to C_{13} chains and the apparent upper limit at C_{17} products are particularly striking. Longer than C_{17} chains have not been observed experimentally. Interestingly, the C_{12} products in this group originate from an unexpected radical dimerization of MS 128.093, a C_6 compound mentioned earlier (Figure 8). Hydrogen abstraction from the aldehyde functionality of this compound by hydroxyl radicals generates the corresponding C_6 radical, which subsequently dimerizes to form the C_{12} α, ω-diacid (MS 253.909, Figure 10). Similarly, the C_{16} product (MS 306) arises from a partially hydrogenated C_8 monomer. In this case, aldehyde hydrogen abstraction by hydroxyl radicals produces a C_8 radical that dimerizes to yield an α, ω-dicarboxylic acid containing an unsaturated diketone functionality. These findings provide valuable insights into the radical-driven pathways that govern the formation of higher-order organic products in this system.

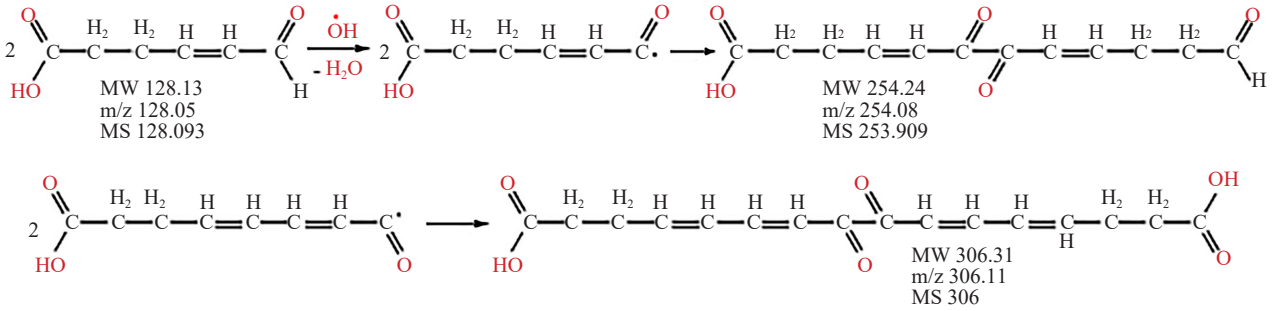

Figure 10. C_6 and C_7 radicals are dimerized to form C_{12} and C_{14} derivatives, respectively

A C_{14} dimer originating from the C_7 MS 140 monomer could not be found, but a coupling product between a hydrogenated C_6 and C_7 monomer radical was identified, yielding the C_{13} di-carboxylic acid diketone MS 272 (Figure 11).

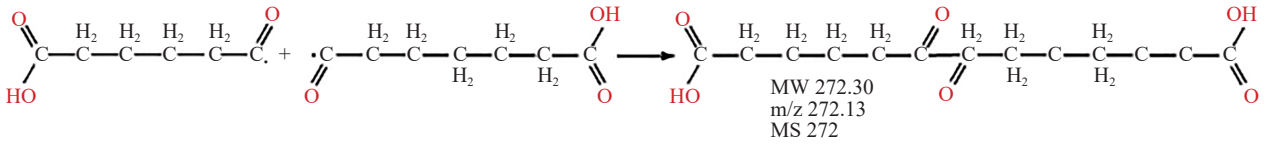

Figure 11. Coupling of C_6 and C_7 radicals yielding the C_{13} tridecanedioic acid-6,7-diketone MS 272

A coupling of C_8 and C_9 radicals forms the linear C_{17} heptadecanedioic acid-8,9-diketone MS 328, the longest carbon chain product identified in this system, see Figure 12.

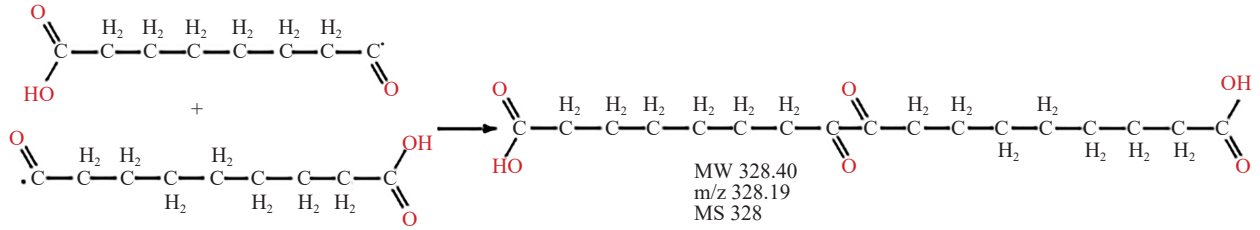

Figure 12. C_8 and C_9 radicals form the C_{17} α, ω-heptadecanoic acid-8,9-diketone MS 328

An unsaturated, partially hydrolyzed C_8 α, ω-hydroxylic acid keto radical, derived from complex **8**, undergoes dimerization to form the C_{16} unsaturated diacid-diketone-alcohol (MS 342), as illustrated in Figure 13.

In addition to this product, three closely related C_{16} organics are observed in the MALDI-TOF spectrum:

(1) A derivative with an additional hydroxyl group (MS 358).

(2) A compound featuring exclusively single carbon-carbon bonds and one extra hydroxyl group (MS 378).

(3) A fully hydrogenated version of the MS 378 compound, where the two ketone groups are reduced to hydroxyl groups, results in MS 382.

These findings highlight the diversity of C_{16} compounds generated within this system, reflecting the intricate interplay of radical dimerization, partial hydrolysis, and hydrogenation processes.

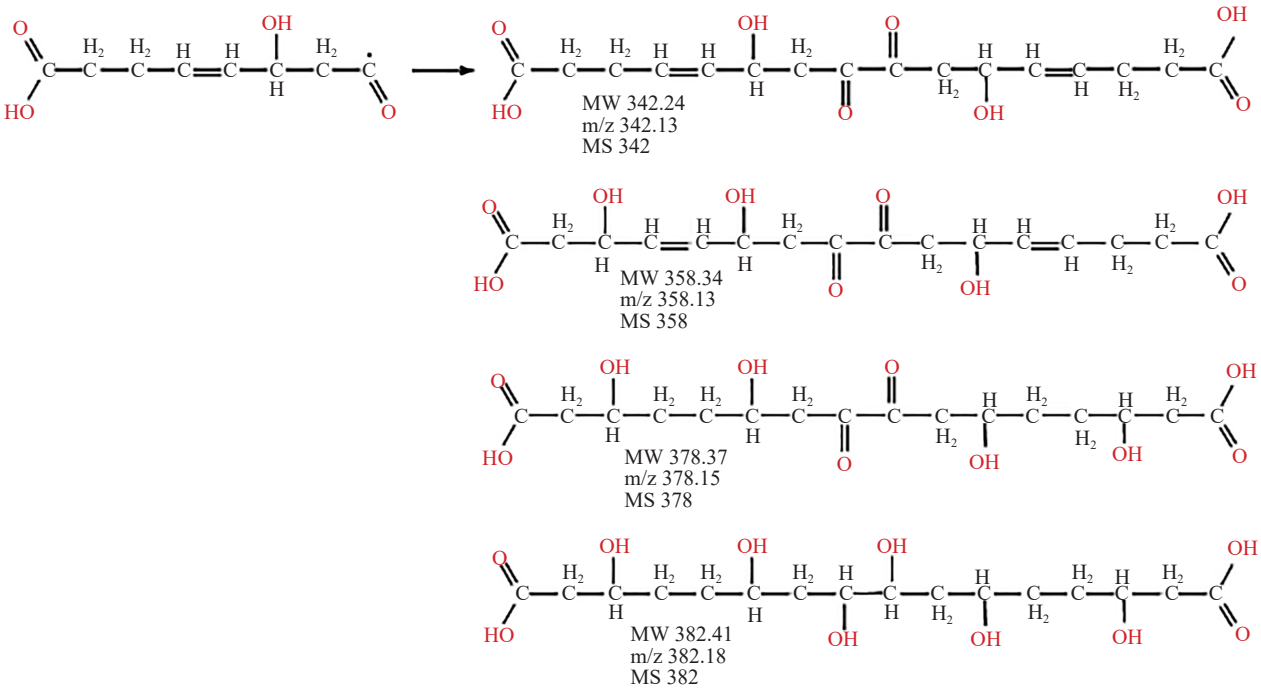

Figure 13. Formation of linear C_{16} oxygenated compounds, derivatives of the α, ω-hexa-decanedioic acid, by dimerization of C_8 carbonyl radicals originating from complex **24**

2.9 *Coupling of C_9 products with 2-phenyl indole radicals*

A third class of compounds produced by our photocatalytic system arises from radical-induced couplings between C9 oxygenated keto radicals and PI radicals, yielding MS 407 and MS 423 (Figure 14). The formation of these products aligns with the expected availability of PI radicals, as evidenced by the previously described radical oligomerization of PI during system operation.[1]

This class also includes two additional products, MS 457.947 and MS 474.12, which result from the coupling of related C_9 radicals with 5-position chlorinated PI radicals (Figure 15). Notably, the coupling process appears to favor C_9 acid/alcohol unsaturated chain keto radicals over shorter counterparts (C_6-C_8). This preference may be attributed to the longer half-life of C_9 radicals.

Among higher molecular weight products are:

MS 574.952: PI trimer.

MS 765.985: PI tetramer.

MS 956.990: Hydrogenated PI pentamer.

MS 1,148.001: Hydrogenated PI hexamer.

These observations underscore the complexity and richness of the photocatalytic system in generating diverse

organic products through a combination of radical coupling, oligomerization, hydrolysis, and hydrogenation processes.

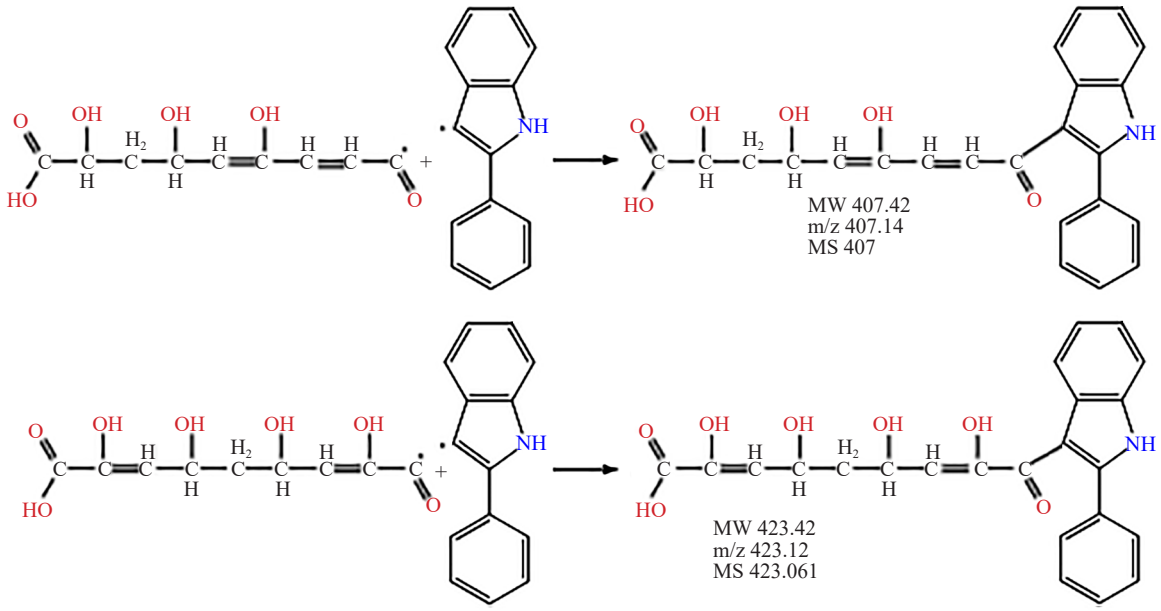

Figure 14. Reaction of C_9 radicals with PI radicals

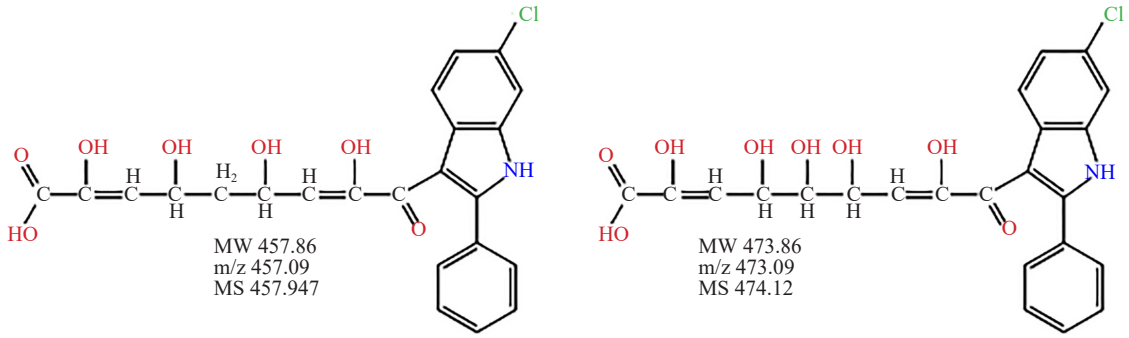

Figure 15. Coupling products of C_9 radicals with chlorinated PI

3. Experimental

$(PI)_2TiCl_4$ was prepared following a published procedure.[1]

MALDI-TOF MS Spectra: Recorded with a Bruker instrument run with Daltonics autoflexR maX Analysis software. Solid samples chosen for analysis were suspended in CH_2Cl_2.

4. Conclusion

The production of C_6-C_{17} oxygenated hydrocarbons from organotitanium compounds marks a significant advancement in organotitanium chemistry and artificial photosynthesis. This study demonstrates that finely tuned titanium-based catalysts enable the efficient formation of valuable hydrocarbons under mild conditions, leveraging titanium's unique stability and reactivity.

By directly synthesizing critical chemical intermediates from CO_2 and water, this method offers a cleaner, more

sustainable alternative to petrochemical processes. Its ability to control hydrocarbon chain length and functionalization makes it highly versatile for producing biofuels, lubricants, and specialty chemicals.

Future research will focus on optimizing catalyst performance, enhancing efficiency, and scaling up for industrial applications. This work advances artificial photosynthesis technologies with broader implications for carbon-neutral industrial processes and renewable energy integration.

Author contributions

GGA wrote this manuscript with contributions from both authors. GGA suggested this study and interpreted the experimental data. MP performed the experimental work and chose the analytical tools.

Acknowledgments

The authors acknowledge the valuable suggestions from the peer reviewers. There has not been any funding for this study.

Conflict of interest

The authors declare no competing financial interest.

References

[1] Paraskevas, M.; Arzoumanidis, G. G. *Fine Chem. Eng*. **2024,** *5*, 369-396.
[2] Godemann, C.; Dura, L.; Hollmann, D.; Grabow, K.; Bentrap, U.; Jiao, H.; Schulz, A.; Brückner, A.; Beweries, Y. *Chem. Commun.* **2015,** *51*(14), 3065-3068.
[3] Godemann, C.; Hollmann, D.; Kessler, M.; Jiao, H.; Spannenberg, A.; Brückner, A.; Beweries, T. *J. Am. Chem. Soc.* **2015,** *137*, 16187-16195.
[4] Nakajima, T.; Tamaki, Y.; Ueno, K.; Kato, E.; Noshikawa, T.; Ohkubo, K.; Yamazaki, Y.; Morimoto, T.; Ishitani, O. *J. Am. Chem. Soc.* **2016,** *138*(42), 13818-13821.
[5] Eidsvag, H.; Bentouba, S.; Vajeeston, P.; Yohi, S.; Velauthapillai, D. *Molecules*. **2021,** *26*(7), 1687-1727.
[6] Kitano, M.; Tsujimaru, K.; Anpo, M. *Top Catal.* **2008,** *49*(1), 4-17.
[7] Nosaka, Y.; Nosaka, A. *ACS Energy Lett.* **2016,** *1*, 356-359.
[8] Arzoumanidis, G. G. *Fine Chem. Eng.* **2023,** *4*, 147-174.
[9] Wang, T.-H.; Navarrete-Lopez, A. M.; Li, S.; Dixon, D. A.; Gole, J. L. *J. Phys. Chem. A.* **2010,** *114*(28), 7561-7570.
[10] Dauth, A.; Love, J. A. *Chem. Rev.* **2011,** *111*, 2010-2042.
[11] Bailey, G. A.; Fogg, D. E. *ACS Catal.* **2016,** *6*, 4962-4971.
[12] Dopke, N. C.; Treichel, P. M.; Vestling, M. M. *Inorg. Chem.* **1998,** *37*(6), 1272-1277.
[13] Fan, Y.; Bao, J.; Shi, L.; Li, S.; Lu, Y.; Liu, H.; Wang, H.; Zhong, L.; Sun, Y. *Catal. Lett.* **2018,** *148*, 2274-2282.